HHS Public Access

Author manuscript

Ophthalmic Surg Lasers Imaging Retina. Author manuscript; available in PMC 2015 March 29.

Published in final edited form as:

Ophthalmic Surg Lasers Imaging Retina. 2014 ; 45(5): 469–473. doi:10.3928/23258160-20140908-01.

Early Structural Anomalies Observed by High-Resolution Imaging in Two Related Cases of Autosomal-Dominant Retinitis Pigmentosa

Sung Pyo Park, MD, PhD, **Winston Lee, MD**, **Eun Jin Bae, MD**, **Vivianne Greenstein, MD**, **Bum Ho Sin, MD**, **Stanley Chang, MD**, and **Stephen H. Tsang, MD, PhD**

Department of Ophthalmology, Kangdong Sacred Heart Hospital, Hallym University Medical Center, Seoul, South Korea (SPP, EJB, BHS); the Department of Ophthalmology, Columbia University, New York, New York (SPP, WL, VG, SC, SHT); and the Department of Pathology and Cell Biology, Columbia University, New York, New York (SHT)

Abstract

The authors report the use of adaptive-optics scanning laser ophthalmoscopy (AO-SLO) to investigate RHO, D190N autosomal-dominant retinitis pigmentosa in two siblings (11 and 16 years old, respectively). Each patient exhibited distinct hyperautofluorescence patterns in which the outer borders corresponded to inner segment ellipsoid band disruption. Areas within the hyperautofluorescence patterns exhibited normal photoreceptor outer segments and retinal pigment epithelium. However, AO-SLO imaging revealed noticeable spacing irregularities in the cone mosaic. AO-SLO allows researchers to characterize retinal structural abnormalities with precision so that early structural changes in retinitis pigmentosa can be identified and reconciled with genetic findings.

INTRODUCTION

Retinitis pigmentosa (RP) is a family of inherited retinal dystrophies defined clinically by the progressive degeneration of photoreceptors, which results from mutations in rhodopsin (RHO) in approximately 10% of RP cases.[1–6] The substitution of asparagines (D) for aspartate (N) at position 190 (D190N) within rhodopsin disrupts intermolecular stability and impairs phototransduction.[7,8]

Adaptive-optics scanning laser ophthalmoscopy (AO-SLO) is a new technology that corrects optical aberrations, which allows for the visualization of retinal microstructures.[9,10] Our AO-SLO prototype utilizes a dual-liquid crystal on silicon spatial light modulator (LCOS-SLM) as a wavefront corrector. Photoreceptors can be imaged at higher resolution than is possible when using a deformable mirror or single LCOS-SLM.

Address correspondence to Stephen H. Tsang, MD, PhD, Bernard and Shirlee Brown Glaucoma Laboratory, Edward S. Harkness Eye Institute, Columbia University, 160 Fort Washington Avenue, Room 513, New York, NY 10032; 212-342-1186; fax: 212-342-7942; gene.targeting@gmail.com.

The remaining authors have no financial or proprietary interest in the materials presented herein.

Structural changes to cones in RHO, D190N autosomal-dominant retinitis pigmentosa (ADRP) result in the abnormal accumulation of parafoveal hyperau-tofluorescence.[8,11–14] This report reexamines two siblings with RHO, D190N ADRP using AO-SLO to characterize the morphological, structural, and functional status of the cone mosaic.[15]

CASE REPORT

The direct DNA sequencing of blood serum led to the diagnosis of both siblings (aged 11 and 16 years, respectively) with RHO, D190N ADRP. Each subject was prescribed oral vitamin A supplements (15,000 IU/day).[16] Funduscopic examinations revealed mild, inferonasal migration of the retinal pigment epithelium (RPE) in case 2 (data not shown). Scanning laser ophthalmoscopy (HRA; Heidelberg Engineering, Heidelberg, Germany) showed pathologic hyperautofluorescence forming an arc pattern (Figure 2A) at the inferior fovea in case 2; an annulus shape was observed in case 1 (Figure 1A).

Spectral-domain optical coherence tomography (SD-OCT) (Spectralis SD-OCT; Heidelberg Engineering, Heidelberg, Germany) revealed preserved retinal-layer architecture within the area of hyperautofluorescence in each case (Figures 1B and 2D). Disruption of the inner segment ellipsoid band (ISe) outside the margin of hyperautofluorescence was also detected by SD-OCT. In both cases, measurements of outer segment and RPE thickness showed abnormal thinning throughout the hyperautofluorescent ring (Figures 1D and 2C). Microperimetry (MP-1; Nidek Technologies, Padova, Italy) showed full visual function within this same area; however, pockets of decreased sensitivity were observed as well (Figures 1C and 2B).

Selected AO-SLO images obtained at distances of 0.5, 1.0, and 1.5 mm from the fovea are presented with corresponding images from age-matched controls. The cone mosaic in normal subjects (Figure 1F) appeared as a densely packed, well-ordered matrix. Individual cone cells were visibly discernible from their neighbors. Size differences were observed to increase with eccentricity from the fovea. Images taken within 0.5 mm of the fovea appeared to be more densely populated with noticeably smaller cones than images obtained at and beyond 1.0 mm. The cone mosaic in both cases presented here appeared less contiguous (Figures 1E and 2E). Many cones were not individually discernible and appeared misshapen in comparison to those of normal subjects. Overall spacing between individual cones also appeared to increase (Figures 1E and 2E, white arrowheads).

DISCUSSION

Autosomal-dominant RHO, D190N is often associated with rod-cone degeneration. A parafoveal ring of hyperautofluorescence that represents the accumulation of lipofuscin, the byproduct of photoreceptor outer segment dysgenesis, is found in 59% of RP cases.[11–14,17–21] This ring is observed to circumscribe preserved RPE and cone photoreceptors, allowing for the preservation of visual function in many cases.[19] Notably, scotopic visual field testing has shown decreased rod sensitivity within areas of hyperautoflurescence.[22] Rod photoreceptors die first in RP, so any preserved visual function will eventually derive entirely from cone photoreceptors. Most cellular defects, including

RHO, D190N, occur in rod-specific proteins, which leads to night blindness in the early stages of RP.

The massive loss of rods affects the regulation of metabolic pathways, particularly insulin and mTOR signaling in cones, resulting in cell death.[23] Given the crucial and physiologically sensitive status of cones throughout the long course of RP, we sought to examine the morphological features of cones within related patients at two different time points of RHO, D190N RP progression.

Although the structural presence of photoreceptors has been linked to the presence of an ISe band detectable by SD-OCT,[11] Greenstein et al reported possible structural and functional abnormalities within the areas of hyperautofluorescence in RP patients.[24] Similar findings were reported in achromatopsia and cone dystrophy, leading to the suggestion that a normal ISe appearance can mask abnormal cone function.[25] We used AO-SLO to investigate the structural implications of ISe appearance in areas of hyperautofluorescence and the related effects on cone-mediated visual function.

Each patient exhibited normal best corrected visual acuity within the preserved portion of the visual field. Results from MP-1 and SD-OCT measurements supported normal visual function and structural integrity within the area of hyperautofluorescence in both cases. Due to the small size of foveal cones, accurate AO-SLO imaging of cones in the fovea was not possible with our instrument.

While mild disruptions appear as dark spaces throughout the cone mosaics of healthy patients, these were found more frequently in the cases presented here. Analogous findings were described in a previous study that examined a family of patients afflicted with neurogenic muscle weakness, ataxia, and retinitis pigmentosa disease.[26] Immunofluorescence studies on the S334ter-3 transgenic mouse, a model for human RP, showed cone cell remodeling that involved the shortening of cone outer segments.[27] This pattern was attributed to abnormal cone spacing. Using MP-1 technology, Yoon et al[26] found that dark, patchy regions of the cone mosaic corresponded to disturbances in the involved portion of the visual field. Our MP-1 results showed normal functioning at the foveal center and reduced function at various points within and beyond the area of hyperautofluorescence. Such structural disruptions may thus serve as early markers of functional changes.

Our structural observations of consanguineous RP cases affected by the RHO, D190N mutation suggest that the morphological condition of cones within and beyond the hyperautofluorescent ring may appear unaffected when viewed using standard ophthalmic imaging modalities but not when observed through AO-SLO. Similar findings were reported in RP patients and murine models carrying the more prevalent P23H RHO mutation.[28,29] Such findings may provide preliminary evidence for a structural-then-functional model of disruption in RP; however, large-scale studies will be necessary for such generalized conclusions.

Mutation-specific reports such as this one allow researchers to correlate varying phenotypic manifestations with mutations common to several genetic diseases. Our study provides high-

quality images of the retinal microstructure at early and advanced stages of ADRP, which may elucidate the therapeutic potential of preserving or rescuing cone cells for restoring vision in other retinal diseases.

Acknowledgments

The authors thank Canon (Tokyo, Japan) for technical support with the adaptive-optics scanning laser ophthalmoscopy instrument.

Supported by the NIH/NEI; R01 EY018213 (SHT); Foundation Fighting Blindness; an unrestricted grant to the Department of Ophthalmology, Columbia University, from Research to Prevent Blindness; Foundation Fighting Blindness; Schneeweiss Stargardt Fund; and The Starr Foundation. Dr. Tsang is a Fellow of the Burroughs Welcome Program in Biomedical Sciences, and has been supported by the Bernard Becker-Association of University Professors in Ophthalmology-Research to Prevent Blindness Award, Foundation Fighting Blindness, Dennis W. Jahnigen Award from the American Geriatrics Society, Crowley Family Fund, Joel Hoffman Fund, Gale and Richard Siegel Stem Cell Fund, Charles Culpeper Scholarship, Schneeweiss Stem Cell Fund, Irma T. Hirschl Charitable Trust, Bernard and Anne Spitzer Stem Cell Fund, Barbara & Donald Jonas Family Fund, and Professor Gertrude Rothschild Stem Cell Foundation.

References

1. Blanks JC, Adinolfi AM, Lolley RN. Photoreceptor degeneration and synaptogenesis in retinal-degenerative (rd) mice. J Comp Neurol. 1974; 156(1):95–106. [PubMed: 4836657]
2. Bowes C, Li T, Danciger M, Baxter LC, Applebury ML, Farber DB. Retinal degeneration in the rd mouse is caused by a defect in the beta subunit of rod cGMP-phosphodiesterase. Nature. 1990; 347(6294):677–680. [PubMed: 1977087]
3. Hernandez-Rodriguez EW, Sanchez-Garcia E, Crespo-Otero R, Montero-Alejo AL, Montero LA, Thiel W. Understanding rhodopsin mutations linked to the retinitis pigmentosa disease: a QM/MM and DFT/MRCI study. J Phys Chem B. 2012; 116(3):1060–1076. [PubMed: 22126625]
4. Rivolta C, Sharon D, DeAngelis MM, Dryja TP. Retinitis pigmentosa and allied diseases: numerous diseases, genes, and inheritance patterns. Hum Mol Genet. 2002; 11(10):1219–1227. [PubMed: 12015282]
5. Filipek S, Stenkamp RE, Teller DC, Palczewski K. G protein-coupled receptor rhodopsin: a prospectus. Annu Rev Physiol. 2003; 65:851–879. [PubMed: 12471166]
6. Palczewski K, Kumasaka T, Hori T, et al. Crystal structure of rhodopsin: A G protein-coupled receptor. Science. 2000; 289(5480):739–745. [PubMed: 10926528]
7. Okada T, Terakita A, Shichida Y. Structure-function relationship in G protein-coupled receptors deduced from crystal structure of rhodopsin. Tanpakushitsu Kakusan Koso. 2002; 47(8 Suppl): 1123–1130. [PubMed: 12099033]
8. Janz JM, Farrens DL. Assessing structural elements that influence Schiff base stability: mutants E113Q and D190N destabilize rhodopsin through different mechanisms. Vision Res. 2003; 43(28): 2991–3002. [PubMed: 14611935]
9. Zhang Y, Poonja S, Roorda A. MEMS-based adaptive optics scanning laser ophthalmoscopy. Opt Lett. 2006; 31(9):1268–1270. [PubMed: 16642081]
10. Zhang Y, Roorda A. Evaluating the lateral resolution of the adaptive optics scanning laser ophthalmoscope. J Biomed Opt. 2006; 11(1):014002. [PubMed: 16526879]
11. Lima LH, Cella W, Greenstein VC, et al. Structural assessment of hyperautofluorescent ring in patients with retinitis pigmentosa. Retina. 2009; 29(7):1025–1031. [PubMed: 19584660]
12. Robson AG, Michaelides M, Saihan Z, et al. Functional characteristics of patients with retinal dystrophy that manifest abnormal parafoveal annuli of high density fundus autofluorescence; a review and update. Doc Ophthalmol. 2008; 116(2):79–89. [PubMed: 17985165]
13. Popovic P, Jarc-Vidmar M, Hawlina M. Abnormal fundus auto-fluorescence in relation to retinal function in patients with retinitis pigmentosa. Graefes Arch Clin Exp Ophthalmol. 2005; 243(10): 1018–1027. [PubMed: 15906064]

14. Kaushal S, Ridge KD, Khorana HG. Structure and function in rhodopsin: the role of asparagine-linked glycosylation. Proc Natl Acad Sci USA. 1994; 91(9):4024–4028. [PubMed: 8171029]
15. Tsui I, Chou CL, Palmer N, Lin CS, Tsang SH. Phenotype-genotype correlations in autosomal dominant retinitis pigmentosa caused by RHO, D190N. Curr Eye Res. 2008; 33(11):1014–1022. [PubMed: 19085385]
16. Tsang SH, Vaclavik V, Bird AC, Robson AG, Holder GE. Novel phenotypic and genotypic findings in X-linked retinoschisis. Arch Ophthalmol. 2007; 125(2):259–267. [PubMed: 17296904]
17. Robson AG, Saihan Z, Jenkins SA, et al. Functional characterisation and serial imaging of abnormal fundus autofluorescence in patients with retinitis pigmentosa and normal visual acuity. Br J Ophthalmol. 2006; 90(4):472–479. [PubMed: 16547330]
18. Robson AG, Tufail A, Fitzke F, et al. Serial imaging and structure-function correlates of high-density rings of fundus autofluorescence in retinitis pigmentosa. Retina. 2011; 31(8):1670–1679. [PubMed: 21394059]
19. Lima LH, Burke T, Greenstein VC, et al. Progressive constriction of the hyperautofluorescent ring in retinitis pigmentosa. Am J Ophthalmol. 2012; 153(4):718–727. 727 e1–2. [PubMed: 22137208]
20. Aizawa S, Mitamura Y, Hagiwara A, Sugawara T, Yamamoto S. Changes of fundus autofluorescence, photoreceptor inner and outer segment junction line, and visual function in patients with retinitis pigmentosa. Clin Experiment Ophthalmol. 2010; 38(6):597–604. [PubMed: 20456441]
21. Wakabayashi T, Sawa M, Gomi F, Tsujikawa M. Correlation of fundus autofluorescence with photoreceptor morphology and functional changes in eyes with retinitis pigmentosa. Acta Ophthalmol. 2010; 88(5):e177–183. [PubMed: 20491687]
22. Robson AG, Egan CA, Luong VA, Bird AC, Holder GE, Gitzke FW. Comparison of fundus autofluorescence with photopic and scotopic fine-matrix mapping in patients with retinitis pigmentosa and normal visual acuity. Invest Ophthalmol Vis Sci. 2004; 45(11):4119–4125. [PubMed: 15505064]
23. Bovolenta P, Cisneros E. Retinitis pigmentosa: cone photoreceptors starving to death. Nat Neurosci. 2009; 12(1):5–6. [PubMed: 19107141]
24. Greenstein VC, Duncker T, Holopigian K, et al. Structural and Functional Changes Associated with Normal and Abnormal Fundus Autofluorescence in Patients with Retinitis Pigmentosa. Retina. 2012; 32(2):349–357. [PubMed: 21909055]
25. Hood DC, Zhang X, Ramachandran R, et al. The inner segment/outer segment border seen on optical coherence tomography is less intense in patients with diminished cone function. Invest Ophthalmol Vis Sci. 2011; 52(13):9703–9709. [PubMed: 22110066]
26. Yoon MK, Roorda A, Zhang Y, et al. Adaptive optics scanning laser ophthalmoscopy images in a family with the mitochondrial DNA T8993C mutation. Invest Ophthalmol Vis Sci. 2009; 50(4): 1838–1847. [PubMed: 18997096]
27. Ji Y, Zhu CL, Grzywacz NM, Lee EJ. Rearrangement of the cone mosaic in the retina of the rat model of retinitis pigmentosa. J Comp Neurol. 2012; 520(4):874–888. [PubMed: 22102145]
28. Berson EL, Sandberg MA, Dryja TP. Autosomal dominant retinitis pigmentosa with rhodopsin, valine-345-methionine. Trans Am Ophthalmol Soc. 1991; 89:117–130. [PubMed: 1808803]
29. Machida S, Kondo M, Jamison JA, et al. P23H rhodopsin transgenic rat: correlation of retinal function with histopathology. Invest Ophthalmol Vis Sci. 2000; 41(10):3200–3209. [PubMed: 10967084]

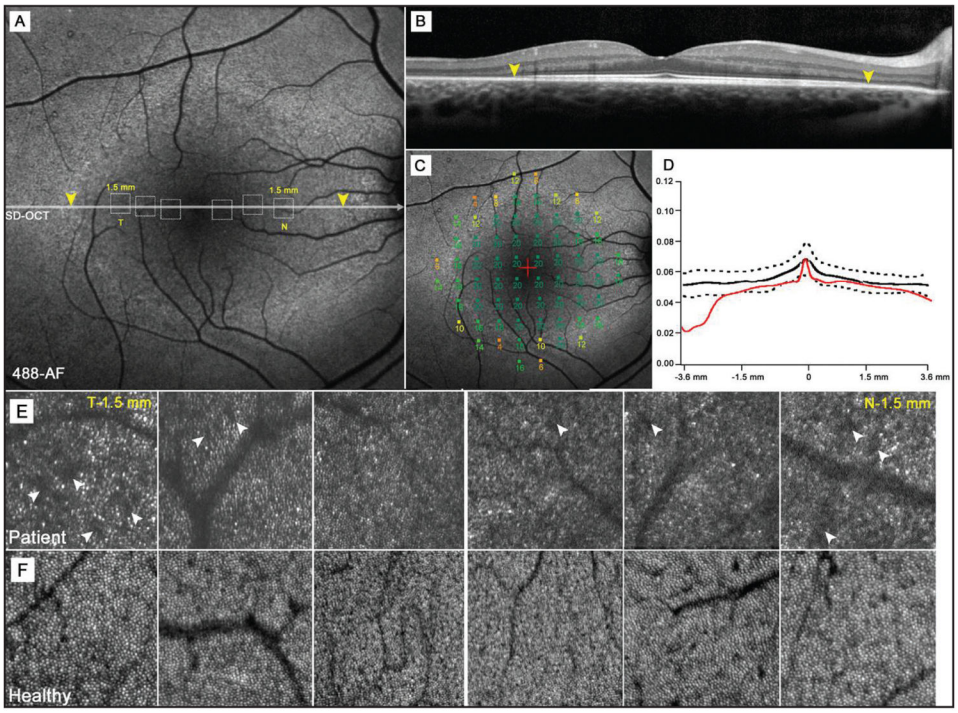

Figure 1.

An 11-year-old boy (case 1) with autosomal-dominant RHO, D190N retinitis pigmentosa. (A) Autofluorescence (AF) image of the right macula exhibiting a hyperautofluorescent ring around the fovea. Yellow arrowheads mark disruption to the inner segment ellipsoid band as detected by spectral-domain OCT (B). Dotted squares represent corresponding areas of adaptive-optics scanning laser ophthalmoscope imaging (AO-SLO) (E). (C) Microperimetry mapping reveals a decline in visual sensitivity (dB) across the hyperautofluorescent ring but no loss in sensitivity in areas within the ring. (D) A plot of photoreceptor outer segment and retinal pigment epithelial thickness across the fovea and retinal thickness in the same area within the ring, showing abrupt thinning beyond the borders of the ring. (E) AO-SLO images taken at positions 0.5, 1.0, and 1.5 mm (temporally and nasally) from the fovea. Corresponding areas are mapped to a 30° AF image (A). (F) AO-SLO images taken within the same retinal positions in an age-matched healthy subject.

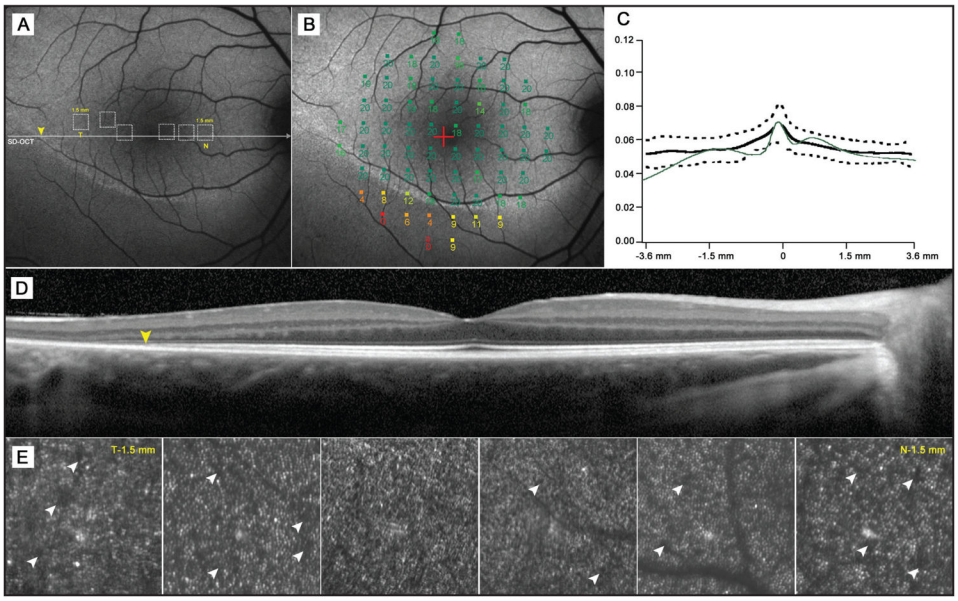

Figure 2.

A 16-year-old boy (case 2) with autosomal-dominant RHO, D190N retinitis pigmentosa. (A) Autofluorescence (AF) image of the right macula showing a hypoautofluorescent, inferiorly concave arc around the fovea. Yellow arrowheads correspond to inner segment ellipsoid band disruption detected by spectral-domain OCT (D). (B) Microperimetry mapping shows similar declines in visual sensitivity (dB) across the hyperautofluorescent arc border; however, the losses in sensitivity within the arc are mild in contrast to case 1. (C) Photoreceptor outer segment and retinal pigment epithelial thickness across the fovea compared to retinal thickness in the same area within the ring and abrupt thinning beyond the borders of the ring. (E) Adaptive optics-scanning laser ophthalmoscope images taken at positions 0.5, 1.0, and 1.5 mm (temporally and nasally) from the fovea with position correspondence observed in the dotted boxes in an AF image (A).